

# Understanding the mechanism of slope failure on a nearby highway tunnel route by different slope stability analysis methods: a case from NE Turkey

Ayberk Kaya<sup>1</sup> · Aykut Akgün<sup>2</sup> · Kadir Karaman<sup>3</sup> · Fikri Bulut<sup>2</sup>

Received: 13 March 2015 / Accepted: 4 July 2015 / Published online: 21 July 2015  
© Springer-Verlag Berlin Heidelberg 2015

**Abstract** The Arakli tunnel is located in the eastern Black Sea region where the most mass movement is observed in Turkey. Following the tunnel entrance portal excavations in basaltic tuffs on nearby the Konakonu residential area, an impending failure occurred. Because of the developed tension cracks and deformations on the ground, five houses and their gardens were damaged completely. The present study aims to investigate the mechanism of the failure. In order to do this, kinematic, limit equilibrium, and numerical stability analyses were carried out. Firstly, the kinematic analyses were performed taking into account the main joint sets for the slopes. The results of the kinematic analyses showed that planar and wedge failures were possible on the portal slope and no failure occurred on the cut slope. However, the limit equilibrium analysis showed that neither the planar nor wedge failures were expected to occur on the portal slope. The numerical stability analyses were performed to determine if circular failure is to occur in the slopes. The Phase<sup>2</sup> programme was used in the numerical analyses, and the Strength Reduction Factors (SRF) of the slopes were determined. According to the numerical stability analyses, the failure mode for the portal slope is composite starting with a circular surface and

following a linear surface and circular for the cut slope. The stability analyses indicated that the failure mechanism was not directly controlled by the joints and might be related to the low strength parameters of the rock mass and joints. Finally, precautions were determined to make the region stable using the Phase<sup>2</sup> programme. After support installation, the SRF values for the portal and cut slopes increased from 1.21 to 1.63 and from 1.32 to 1.71, respectively. These results showed that the proposed support units prevent the effects of failure and were essential for the long-term stability.

**Keywords** Slope stability · Mass movement · Numerical analysis · Support design

## Introduction

Stability analysis of rock slopes is crucial for safety design in geotechnical engineering and open-pit mining. Various methods are performed for evaluation of the slope stability. Kinematic, limit equilibrium, and numerical analyses are widely used by engineers for the designing of safe slopes. The kinematic analysis deals with the motion of the bodies without consideration of the forces that give rise to motion (Kliche 1999). The analysis is generally used in the initial evaluation of the slopes. If the slopes were determined to be unstable based on the kinematic analysis, additional analyses, such as the limit equilibrium method, would be implemented for the evaluation of rock slopes (Karaman 2013). Limit equilibrium analysis takes into account the shear strength along a failure surface, the influences of water pressure, and the effect of external activities, such as seismic accelerations or reinforcing units (Kentli and Topal

✉ Aykut Akgün  
aykut.akgun@ktu.edu.tr

<sup>1</sup> Department of Geological Engineering, Faculty of Engineering, Recep Tayyip Erdogan University, 53100 Rize, Turkey

<sup>2</sup> Department of Geological Engineering, Faculty of Engineering, Karadeniz Technical University, 61080 Trabzon, Turkey

<sup>3</sup> Department of Mining Engineering, Faculty of Engineering, Karadeniz Technical University, 61080 Trabzon, Turkey

2004). Notwithstanding this, it is usually insufficient if the slope fails by a complicated mechanism such as excavation disturbance, discontinuity orientation (Eberhardt 2003). Numerical analyses (e.g. finite element method, finite difference method, and boundary element method) are fulfilled to confirm findings obtained from the kinematic and equilibrium analysis (Gurocak et al. 2008). Because each analysis method considers a different set of geotechnical factors, at least two methods shall be used in the evaluation of rock slopes.

Mass movement in the eastern Black Sea region (EBSR) in Turkey is one of the most frequently observed natural disasters. A number of researchers (e.g. Genc 1993; Bulut et al. 2000; Akgun and Bulut 2007; Akgun et al. 2008; Yalcin and Bulut 2007; Kesimal et al. 2008; Reis 2008; Yalcin 2008; Karsli et al. 2009; Akgun 2011; Nefeslioglu and Gokceoglu 2011; Nefeslioglu et al. 2011; Reis et al. 2012; Alemdag et al. 2013; Karaman et al. 2013; Alemdag et al. 2014; Osna et al. 2014; Topsakal and Topal 2015; Alemdag et al. 2015) have investigated the slope stability problems observed in the EBSR. The mountainous area of the EBSR receives the highest amount of rainfall. Because of the heavy traffic load and topographical conditions of the EBSR, the Turkish General Directorate of Highways authorities decided to construct the Arakli tunnel (Fig. 1). The Arakli tunnel is excavated through the volcanic rocks of the Eocene-aged Kabaköy Formation. Along the tunnel alignment, the lithology of the rocks changes in short distances. Because the entrance portal of the tunnel involves basaltic tuffs, it is the most problematic section of the tunnel. This condition requires an evaluation of tunnel portal slopes with proper analysis techniques chosen. For this reason, the excavation design of the portal and cut slopes taking into account their stability properties contribute to the applicability of the project in terms of its cost, safety, and timing. On the other hand, collapse of the portal slopes may cause the cutting off of traffic and loss of life. The entrance portal section of the Arakli tunnel was planned to excavate on the nearby Konakonu residential area. Excavations with an approximate height of 22 m for the portal and 19 m for the cut slopes triggered a mass movement. This failure damaged five houses, caused the development of cracks on the ground and garden walls, and tilting of fences and trees (Fig. 2). These deformations indicate the existence of an impending failure in the study area. The tension cracks on the ground have retrogressively developed and enlarged by the retrogressive failures. The initial tension cracks close to the slope faces are followed by the next cracks towards the Konakonu residential area. Therefore, detailed geotechnical studies were carried out to understand the mechanism of impending failure and to determine the support design to

make the region stable by means of field and laboratory studies.

## Geology of the study and surrounding area

The study area is located in the northern part of the Eastern Pontides Tectonic Unit, Black Sea Region, Turkey. The Eocene-aged Kabakoy Formation, first described by Guven (1993), shows wide expansion in the study area (Fig. 3). This formation lithologically consists of andesite, basalt, and their pyroclastites. The following volcanic rocks comprising the basaltic and andesitic tuffs, agglomerates, and basalts are encountered in the tunnel alignment. Basaltic tuffs to be driven by the entrance portal section have pale green colours. They contain sporadic pyrite occurrences, and hematization is commonly seen in some places throughout the outcrops. Agglomerates consist of rounded-basalt pyroclastics having diameters of between 2 and 30 cm. Chloritisation is seen as patches in cement material of rock. Basalts are in dark to dark gray colour, and they present a massive texture without any observable weathering products. Basaltic dykes, generally located along faults, are associated with the Kabakoy Formation (Kaya 2008).

The Pliocene-aged Besirli Formation is encountered along the southern part of the study area (Fig. 3). The formation occurs as local outcrops with a thickness of 3–5 m, rests disconformably on the underlying units and comprises breccias and conglomerates that are weakly cemented. Further, coarse-grained sandstone, thickly bedded sandy limestone, and basaltic agglomerates can be seen within this formation (Guvén 1993).

Quaternary recent sedimentary units are reflected by alluvium of the streams, river valley deposits, and slope debris. The widest outcrop of the alluvium can be observed in the Karadere stream valley (Fig. 3). It consists of various materials from block to clay-sized materials. The alluvium's thickness changes in the range of 16 to 28 m. Slope debris are cropped out on slopes in the study area and surroundings and are angled, tabular, and sometimes less rounded in shape depending on the rock types. The amount of sand, silt, and clay is more than the gravel and block elements (Kaya et al. 2011a, b).

## Geotechnical investigations

In order to determine the geotechnical properties of the basaltic tuffs, field and laboratory studies were carried out in the scope of this study. Twelve investigation boreholes (Figs. 3, 4) having a total length of 303 m were drilled so that the discontinuity properties and groundwater level

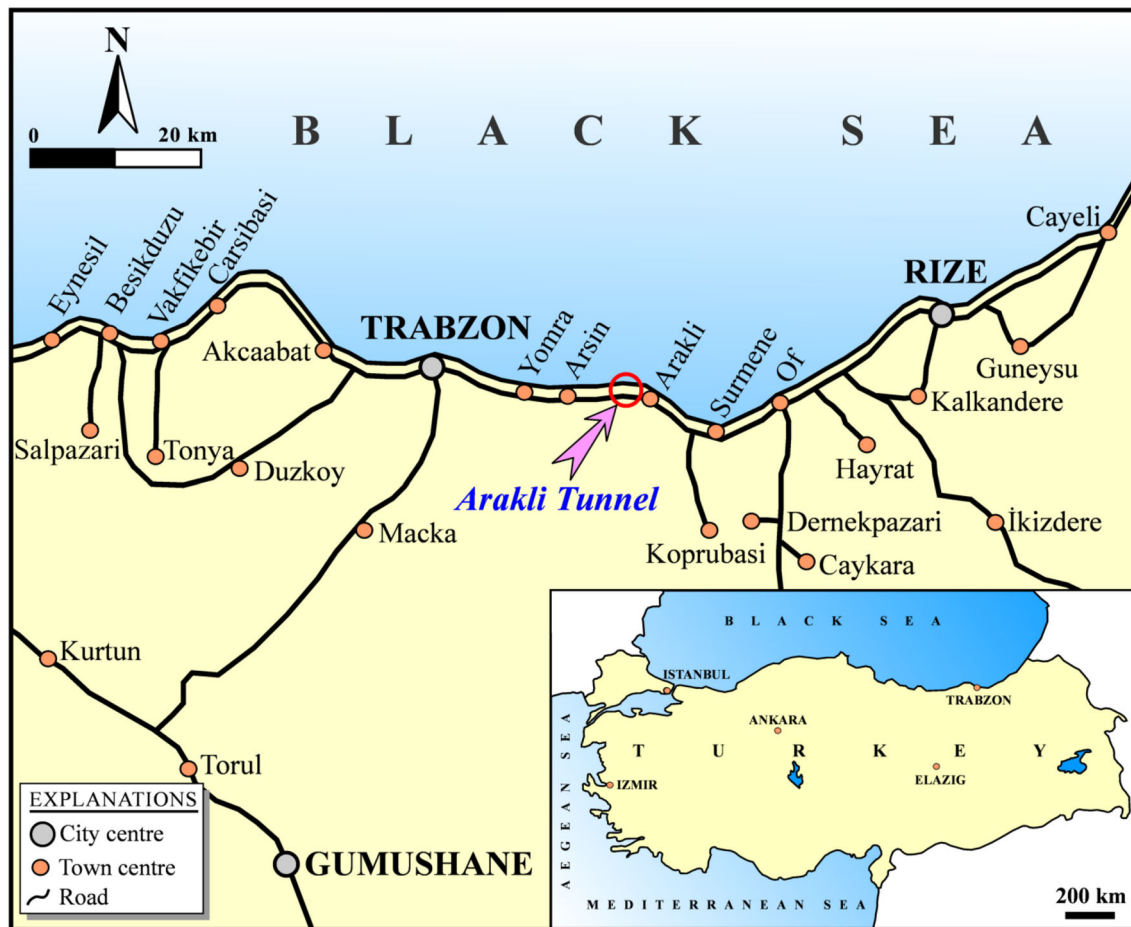


Fig. 1 Location map of the study area

might be identified. Four of them (KTS 1–4) were drilled to explore the properties of the basaltic tuffs located in the entrance portal at the design stage of the Arakli tunnel. The other eight boreholes, denoted by SK 1–8, were drilled for investigating the mechanism of the failure related to the slope excavations.

Laboratory experiments were performed on the rock cores taken from the boreholes. They were implemented according to the methods proposed by ISRM (2007) to determine the physico-mechanical and elastic properties of the basaltic tuffs, including uniaxial compressive strength ( $\sigma_{ci}$ ), point load strength index ( $I_{S(50)}$ ), unit weight ( $\gamma$ ), Young’s modulus ( $E_i$ ), and Poisson’s ratio ( $\nu$ ). Further, the Rock Quality Designation (RQD) values were determined using the method suggested by Deere (1964) and range from 54 to 85 %. Table 1 shows the findings of the laboratory tests.

The quantitative description of the joints in the basaltic tuffs such as orientation, persistence, roughness, spacing, degree of weathering, infilling, and aperture were determined by analyzing the cores in accordance with methods

suggested by the ISRM. According to the ISRM (2007), the joints in the basaltic tuffs are closely spaced with medium persistence, open, undulating, and moderately weathered (Table 2). A total of 178 joint measurements were taken and their orientations were processed by using computer software called Dips v5.1 (Rocscience 2004a), according to the equal-area stereographic projection and dominant joint sets have been determined on the basaltic tuffs (Fig. 5).

The Barton–Bandis failure criterion proposed by Barton and Bandis (1990) was used to calculate the peak shear strength parameters of the joints. Suggested equations for the criterion are given as follows:

$$\phi_r = (\phi_b - 20) + 20 (r/R) \tag{1}$$

$$\tau = \sigma_n \tan \left[ \phi_r + JRC \log \left( \frac{JCS}{\sigma_n} \right) \right] \tag{2}$$

where  $\tau$  shear strength of the joint surface (MPa),  $\sigma_n$  normal stress acting on the joint surface (MPa), JRC joint roughness coefficient, JCS strength of the joint surface (MPa),  $\phi_r$  residual friction angle,  $\phi_b$  basic friction angle,

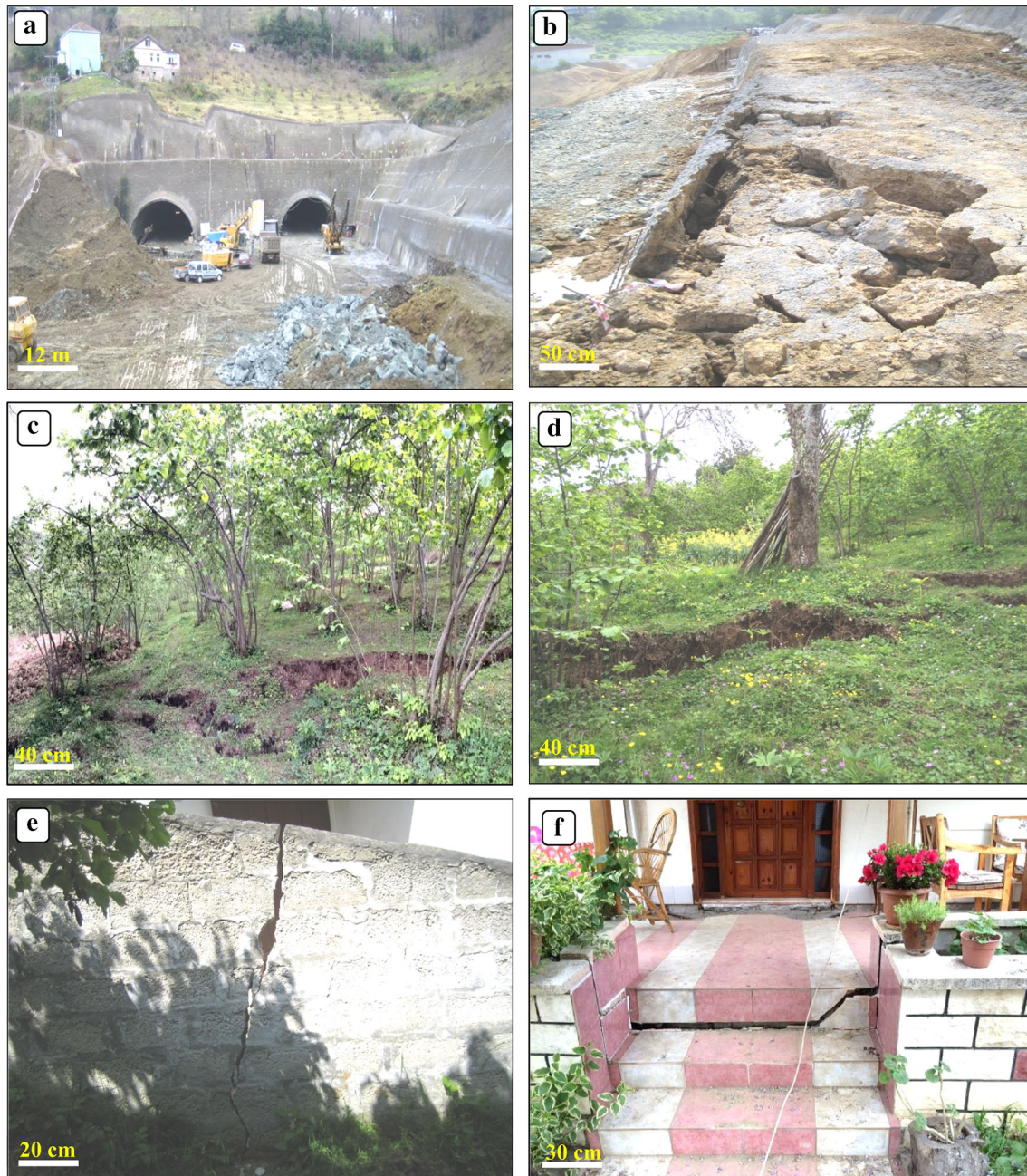


**Fig. 2** **a** Entrance portal of the Arakli tunnel, **b** failure on the cut slope, **c**, **d** tension cracks on the ground, **e** cracks on the garden wall and **f** house stairs formed by the mass movement

$R$  Schmidt rebound value of the dry joint surface, and  $r$  Schmidt rebound value of the wet joint surface.

This method was carried out in two steps. Firstly, the deformation controlled direct shear tests proposed by CANMET (1977) were performed on the block samples having dimensions of  $60 \times 60 \times 10$  mm to determine the  $\phi_b$  value. A  $\tau$ - $\sigma$  graph was drawn using the data obtained from the tests (Fig. 6a), the  $\phi_b$  value was determined to be  $31^\circ$ , and the  $\phi_r$  value was calculated as  $27^\circ$  using Eq. 1.

Secondly, to determine the peak shear strength parameters of the joints, Barton–Bandis failure envelope was drawn (Fig. 6b) using Eq. 2, and by drawing the tangent representing the Mohr–Coulomb failure envelope, the peak friction angle and peak cohesion of the joints were determined as  $41^\circ$  and 32 kPa, respectively. The parameters used in the Barton–Bandis failure criterion are given in Table 3.

The Geological Strength Index (GSI) was derived from the last version of the quantitative GSI chart suggested by

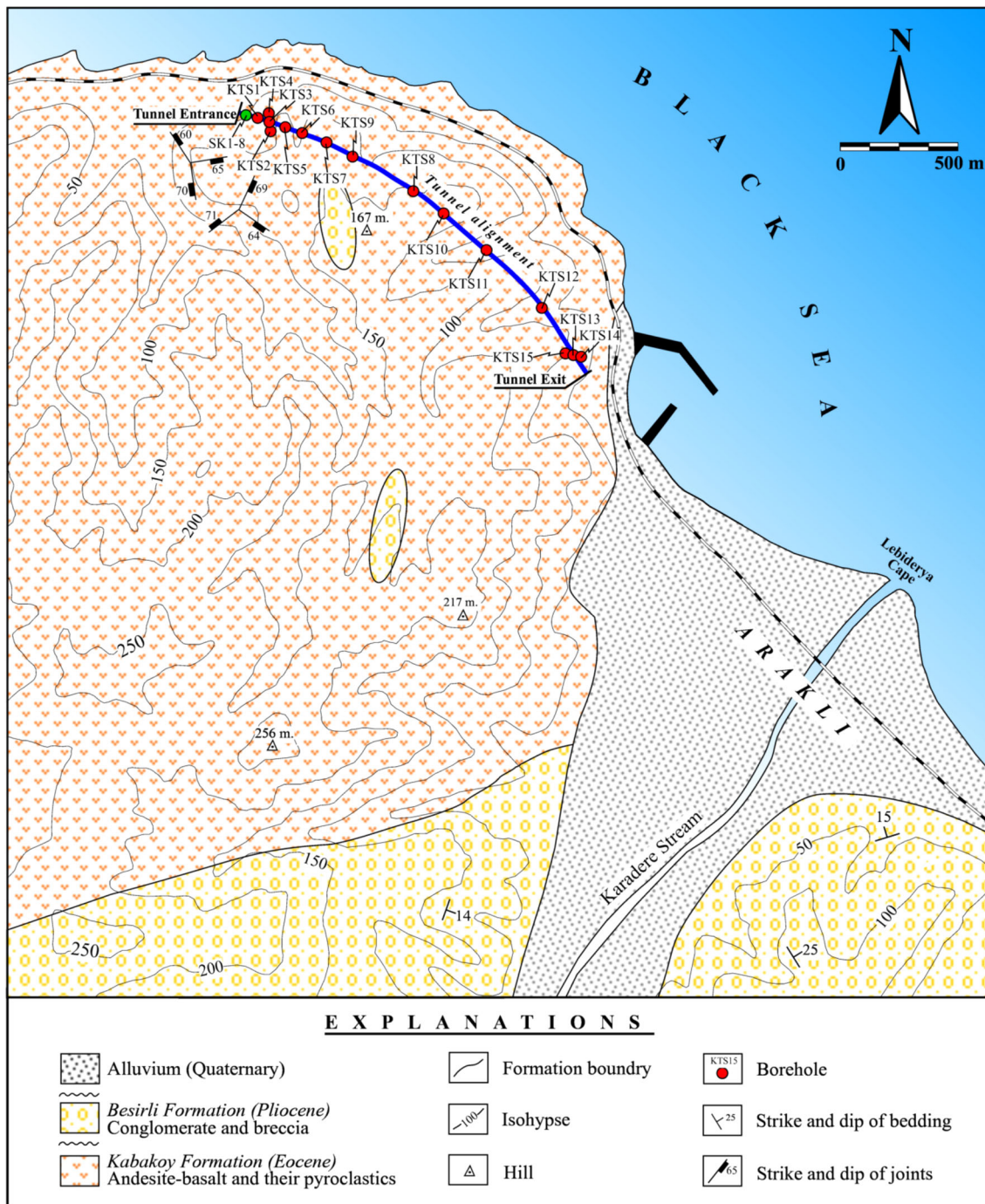


**Fig. 3** Simplified geological map of the close vicinity of the study area (modified from Guven 1993)

Hoek and Marinos (2000). The GSI value of the basaltic tuffs was determined to be 39, and the quality of the rock mass was classified as “Blocky, disturbed/seamy” according to the GSI chart. Rock mass parameters such as Hoek–Brown constants ( $m_b$ ,  $s$ ,  $a$ ), modulus of deformation ( $E_m$ ), uniaxial compressive strength ( $\sigma_{cm}$ ), tensile strength ( $\sigma_{tm}$ ), cohesion ( $c'$ ), and friction angle ( $\phi'$ ) are essential input values for the numerical stability analyses. To

determine the rock mass parameters of the basaltic tuffs, the Hoek–Brown failure criterion was used. The  $m_b$ ,  $s$  and  $a$  constants,  $\sigma_{cm}$ ,  $\sigma_{tm}$ ,  $c'$  and  $\phi'$  values were calculated using the suggested equations by Hoek et al. (2002). Further, the deformation modulus of the basaltic tuffs was determined using the equation of the Hoek and Diederichs (2006). Because mechanical excavation was applied, the value of the disturbance factor ( $D$ ) was considered to be

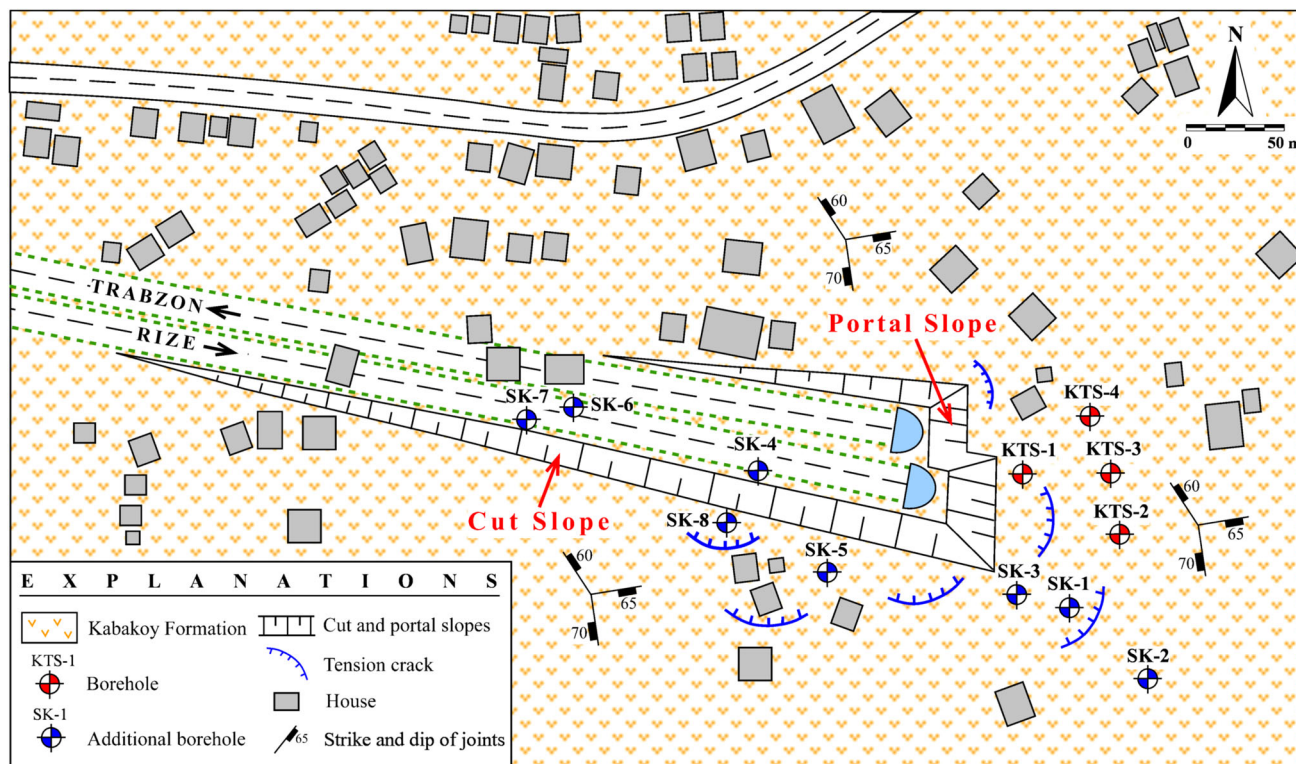


**Fig. 4** Detailed geological map of the entrance section of the Arakli tunnel and its vicinity

**Table 1** Physical, mechanical and elastic properties of the basaltic tuffs

Properties	Min.	Max.	Ave.	SD
Unit weight ( $\gamma$ , kN/m <sup>3</sup> )	18.32	22.16	20.11	1.92
Uniaxial compressive strength ( $\sigma_{ci}$ , MPa)	17.31	19.51	18.58	0.89
Point load strength index ( $I_{S(50)}$ , MPa)	0.39	2.00	0.80	0.15
Young's modulus ( $E_i$ , GPa)	10.22	11.52	10.98	0.65
Poisson's ratio ( $\nu$ )	0.31	0.35	0.33	0.02
Rock quality designation (RQD, %)	54	85	66	5

*Min.* Minimum, *Max.* Maximum, *Ave.* Average, *SD.* Standard deviation

zero. The  $m_i$  constants of the rock material was determined using the Roclab v1.0 (Rocscience 2007) software and was assumed to be 13. The calculated rock mass parameters and equations used in the calculations are listed in Table 4.

### Slope stability analyses

In order to investigate the stability of the slopes within the study area, the kinematic, limit equilibrium, and numerical analyses were conducted. The kinematic analyses were initially applied to specify the possibility of the occurrence of any toppling, wedge, or planar failure. After determination of the discontinuity controlled failure types using

the kinematic analyses, the stability was evaluated by the limit equilibrium analyses. Finally, the numerical stability analyses were performed to determine if the failure in the study area was related to circular or composite failures.

### Kinematic analyses for the portal and cut slopes

The kinematic analyses were applied along the portal and cut slopes having different orientations by taking into account the main joint sets and their friction angle of 41°. The planar, wedge, and toppling failure modes were kinematically inspected using the combined method suggested by Wyllie and Mah (2004). According to the results of the kinematic analyses, a planar failure along the joint

**Table 2** Quantitative description of joints in the basaltic tuffs

Properties	Values
Joint set number	3 + random
Joint orientation	J1: 60/65 J2: 65/173 J3: 70/268
Joint spacing (cm)	15.4 <sup>a</sup> 5.4–55.2)
Persistence (m)	9.8 <sup>a</sup> (5.5–27.5)
Aperture (mm)	1.2 <sup>a</sup> (1.0–19.5)
Infilling	<5 mm soft clay
Roughness	Rough, undulating
Weathering	Moderately weathered
Groundwater condition	Dripping

<sup>a</sup> Average

set J3 and a wedge failure along the intersection of the joint sets J2 and J3 are expected to occur on the portal slope (Fig. 7a). However, no failure is expected to occur on the cut slope (Fig. 7b). Because of the planar and wedge failures hazard on the portal slope, the limit equilibrium analysis was implemented to check these failures. The parameters used in the analyses and results are given in the Fig. 7 and Table 5.

**Limit equilibrium analyses for the portal slopes**

Kinematic analysis does not consider any external forces acting on a slope forming material, slope height, or significant geotechnical elements. Thus, slope stability is

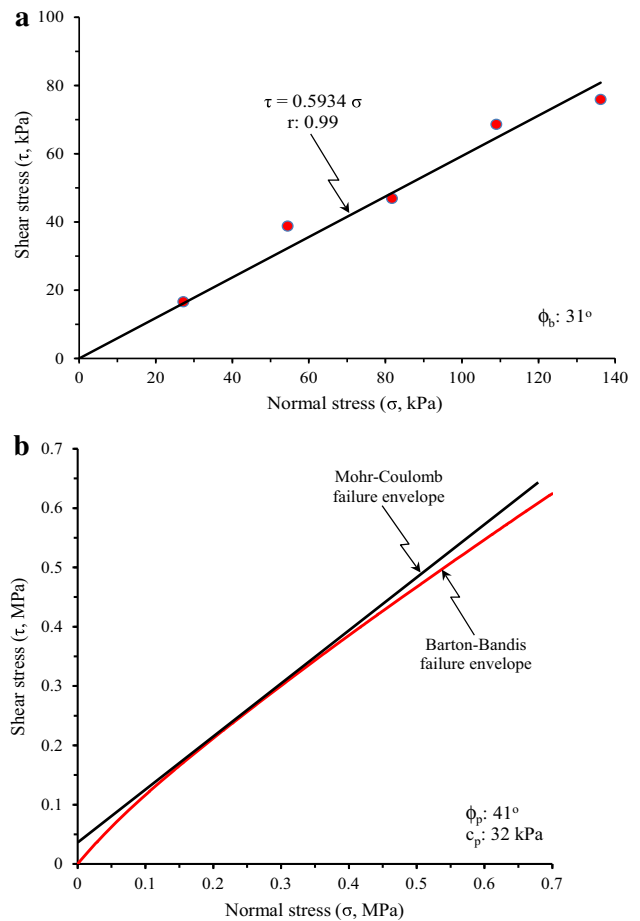


**Fig. 6**  $\sigma$ - $\tau$  Graphs for the **a**  $\phi_b$  and **b**  $\phi_p$  and  $c_p$  values of joints in the basaltic tuffs

**Fig. 5** Equal-area stereographic projection of the joint sets in the basaltic tuffs

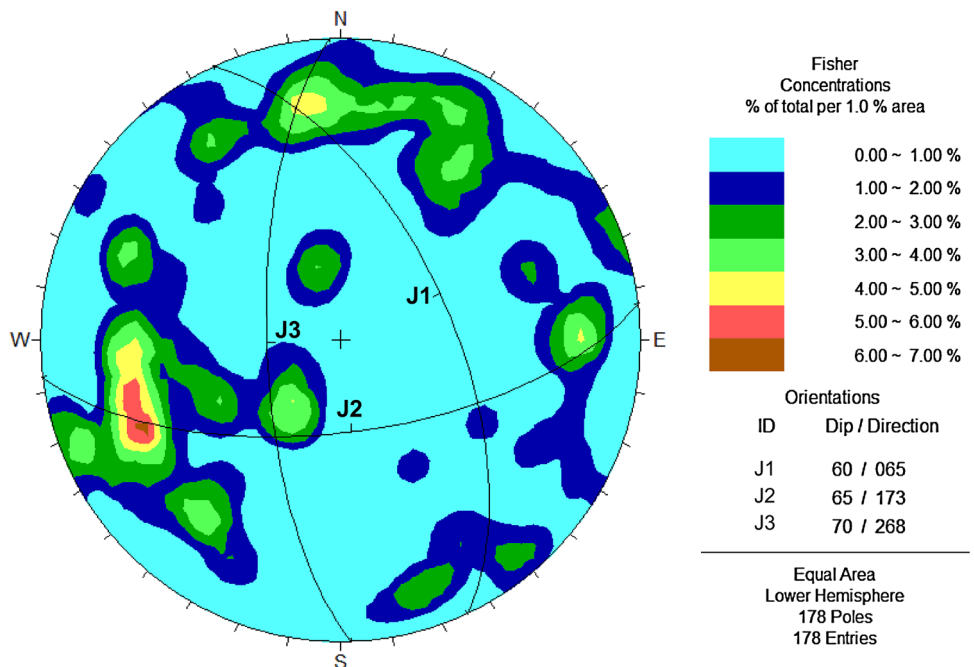


**Table 3** The parameters used in the Barton–Bandis failure criteria and  $\phi_p$  and  $c_p$  values

Input parameters	Value of parameters
Basic friction angle ( $\phi_b$ , °)	31
Dry Schmidt rebound ( $R$ )	36
Wet Schmidt rebound ( $r$ )	28
Residual friction angle ( $\phi_r$ , °)	27
Joint compressive strength (JCS, MPa)	34
Joint roughness coefficient (JRC)	9
Peak friction angle ( $\phi_p$ , °)	41
Peak cohesion ( $c_p$ , kPa)	32

usually analyzed in geotechnical engineering by limit equilibrium analyses, which provide a direct measure of stability in view of the safety factor (Kentli and Topal 2004).

Limit equilibrium analyses were carried out using the software called RocPlane v2.0 (Rocscience 2004b) and Swedge v4.0 (Rocscience 2004c) for the portal slope having potential planar and wedge failures assessed by kinematic analyses. These computer programmes calculate the safety factor ( $F$ ) using the method of the Hoek and Bray (1981) that considers the influences of cohesion and friction angle of joints. For the stability analyses of the critical slopes adjoining highway roads and critical engineering excavations (i.e. tunnel portal slope, open pit mining, etc.), a safety factor of 1.50 is usually preferred (Turkish General Directorate of Highways 1997). Therefore, a safety factor of 1.50 was considered acceptable for the long-term stability in this study.

When calculating of the  $F$  values, forces such as seismic coefficients and other external forces were not included into the analysis because the mass movement in the study area was not triggered by the earthquake. As a result, the  $F$  values of the planar and wedge failure conditions were determined to be 1.602 and 4.324, respectively, for saturated conditions. Because the acute angle between the intersection of the joint sets (J2 and J3) and the strike of portal slope was 31°, a narrow and long wedge weighing 49.6 tonnes was formed. Even though wedge failure was kinematically possible, this condition increased the shear resistance against sliding, and caused a higher  $F$  value of 4.324.

It is very clear that the  $F$  values of the portal slope were higher than both the limit equilibrium condition and acceptable  $F$  value of 1.50 for the stability. Therefore, it can be concluded that the failures on the portal slope were not directly controlled by the joint sets and no planar and wedge failures are expected. The results of the limit equilibrium analyses are given in Table 6.

The failure on the slopes could be connected with the circular or composite failures. Thus, in the last stage, the possibilities of the occurrence of these failure modes were investigated using the numerical analyses.

**Numerical stability analyses of the portal and cut slopes**

The kinematic and limit equilibrium analyses sometimes do not work in rock masses having low strength parameters and dense discontinuities with low shear strength. In this case, the circular failures without discontinuity controlled failures, such as planar, wedge, and toppling, or the

**Table 4** The calculated rock mass parameters of the basaltic tuffs

Researchers	Equations	Notes	Equation numbers	Values
Hoek and Diederichs (2006)	$E_m = E_i \left( \frac{1-(D/2)}{1+e^{(60+15D-GSI)/11}} \right)$	MPa	(3)	1637.18
Hoek et al. (2002)	$\sigma_{cm} = \sigma_{ci} \cdot S^a$	MPa	(4)	0.578
	$\sigma_{tm} = -\frac{s \cdot \sigma_{ci}}{m_b}$	MPa	(5)	-0.014
	$m_b = m_i e^{\left(\frac{GSI-100}{28-14D}\right)}$	$m_i$ : 13 $D$ : 0	(6)	1.472
	$s = e^{\left(\frac{GSI-100}{9-3D}\right)}$	$GSI$ : 39	(7)	0.00114
	$a = \frac{1}{2} + \frac{1}{6} \left( e^{-GSI/15} - e^{-20/3} \right)$		(8)	0.512
	$c' = \frac{\sigma_{ci} [(1+2a)s + (1-a)m_b \sigma'_{3n}] (s+m_b \sigma'_{3n})^{a-1}}{(1+a)(2+a) \sqrt{1 + [6am_b (s+m_b \sigma'_{3n})^{a-1}] / [(1+a)(2+a)]}}$	kPa	(9)	164
$\phi' = \sin^{-1} \left[ \frac{6am_b (s+m_b \sigma'_{3n})^{a-1}}{2(1+a)(2+a) + 6am_b (s+m_b \sigma'_{3n})^{a-1}} \right]$	$\sigma'_{3n} = \sigma'_{3max} / \sigma_{ci}$ $\frac{\sigma'_{3max}}{\sigma_{cm}} = 0.72 \left( \frac{\sigma'_{cm}}{\gamma H} \right)^{-0.91}$ $\sigma'_{cm} = \sigma_{ci} \frac{(m_b + 4s - a(m_b - 8s))(m_b/4 + s)^{a-1}}{2(1+a)(2+a)}$	(10)	49.83	



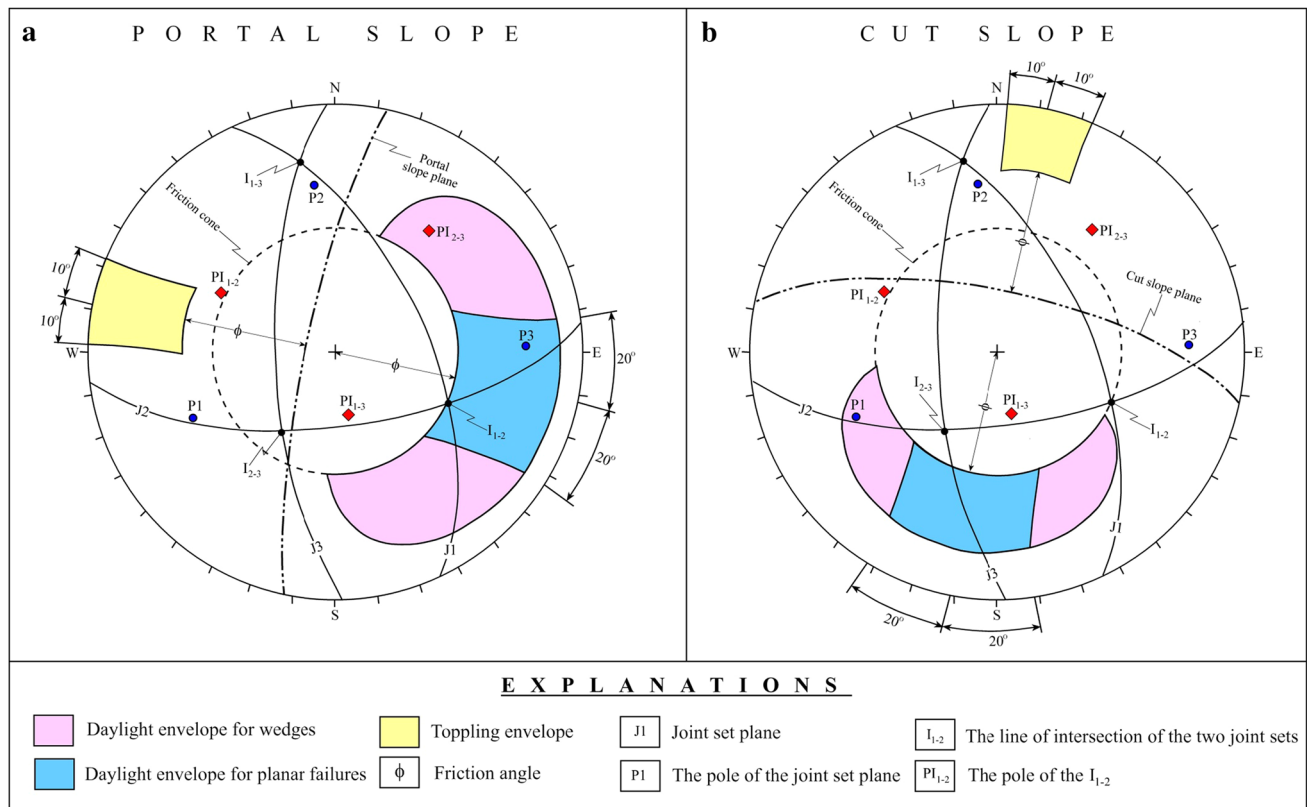


**Fig. 7** Kinematic analyses of the **a** portal and **b** cut slopes

**Table 5** The parameters used in the kinematic analyses and results

Orientation of joint sets	Orientation of intersections	Orientation of slopes	Friction angle	Stability condition		
				Planar failure	Toppling	Wedge failure
J1: 60/65	$I_{1-2}$ : 49/113	Portal face: 80/282	41	Unstable	Stable	Unstable
J2: 65/173	$I_{1-3}$ : 23/349					
J3: 70/268	$I_{2-3}$ : 59/213	Cut slope face: 70/12	41	Stable	Stable	Stable

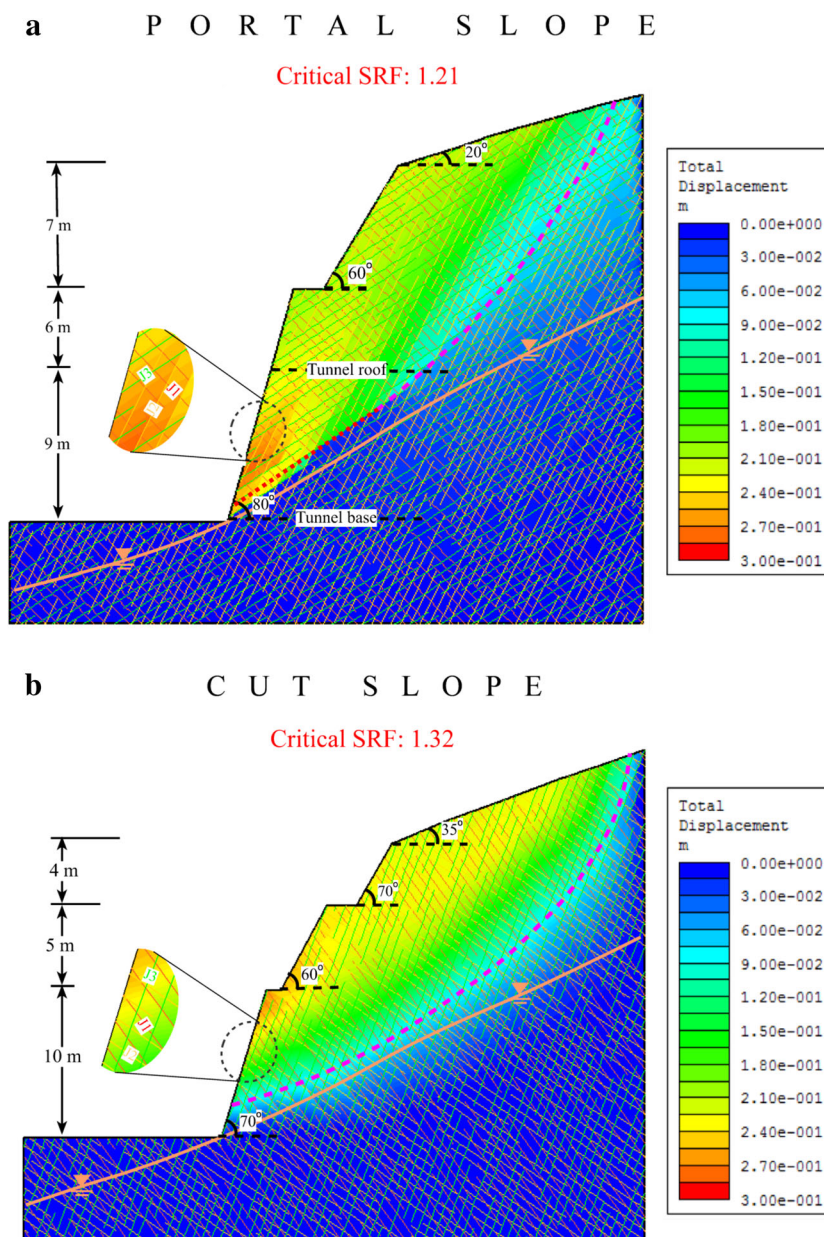
**Table 6** Results of the limit equilibrium and numerical analyses

Slopes	Limit equilibrium analysis			Numerical analyses for unsupported case			Numerical analyses for supported case	
	Probable failure mode	Safety factor ( $F$ )	Stability condition	Probable failure mode	Strength Reduction Factor (SRF)	Stability condition	Strength Reduction Factor (SRF)	Stability condition
Portal slope	Planar	1.602	Stable	Composite (circular+linear)	1.21	Unstable	1.63	Stable
	Wedge	4.324	Stable					
Cut slope	None	–	–	Circular	1.32	Unstable	1.71	Stable

composite failures combined with circular and linear surfaces might occur. The safety of slopes planned to excavate in this kind of rock environment is widely analyzed in geotechnical works using the numerical methods that ensure a direct measure of the stability.

In this study the numerical stability analyses were performed in three steps. Firstly, the geometry of the each slope was introduced into the finite element method (FEM) based software called Phase<sup>2</sup> v7.0 (Rocscience 2008). Phase<sup>2</sup> is a powerful and flexible computer package that

**Fig. 8** Numerical analyses of the **a** portal and **b** cut slopes for the unsupported case



has the Shear Strength Reduction (SSR) method integrated into the FEM and interpretation modules. In the SSR method, the stability factor ( $F$ ) is represented by the Strength Reduction Factor (SRF). The SSR method involves systematic use of FEM to determine a SRF value that brings a slope to the verge of failure. The shear strength parameters of the rock mass are scaled until the stability limit is reached. The SRF value is the ratio between the actual and the model strength at the stability limit (e.g. Griffiths and Lane 1999; Shukra and Baker 2003; Hammah et al. 2006; Li 2007). One of the advantages of the SSR method is that there is no need to guess at determination of critical failure surface. Because of the

advances in computer systems, this method is increasingly used today compared to the past.

After introducing the slope geometry, the material and mass parameters of the basaltic tuffs were described using the geotechnical parameters such as  $\sigma_{ci}$ ,  $\sigma_{cm}$ ,  $\sigma_{ct}$ ,  $\nu$ ,  $\gamma$ ,  $E_m$ ,  $c'$ ,  $\phi'$  values, and groundwater conditions. Furthermore, orientation, length, spacing, and shear strength parameters ( $c_p$  and  $\phi_p$ ) of the joint sets were introduced into each analyzed model as the joint network. The Mohr–Coulomb failure criterion proposed by Mohr (1900) was used in the numerical analyses to define the material and joint properties in order to get more reliable results.

**Fig. 9** Numerical analyses of the **a** portal and **b** cut slopes for the supported case

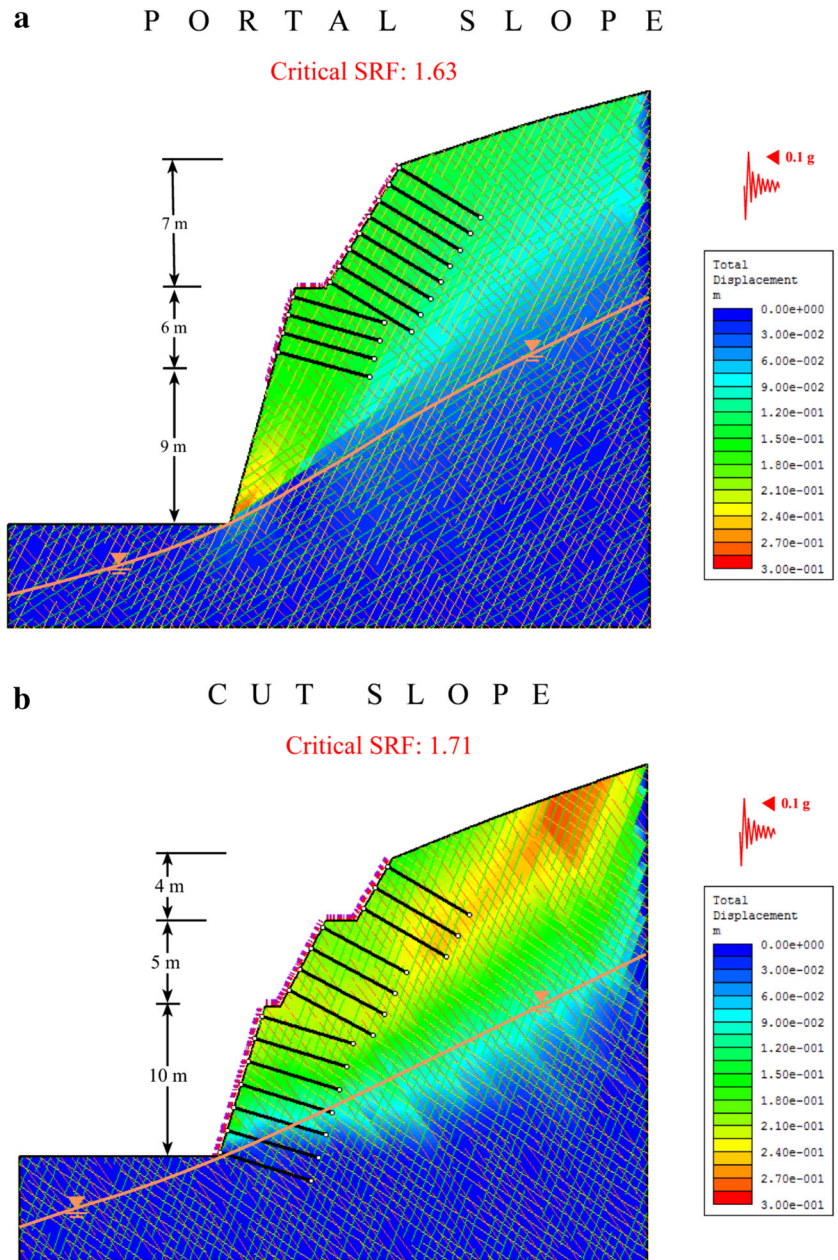


**Table 7** The characteristics of the support units used in the numerical analyses (Turkish General Directorate of Highways 2006)

Properties	Shotcrete	Wire mesh	Rock bolt
Young's modulus ( $E$ , GPa)	20	200	200
Poisson's ratio ( $\nu$ )	0.2	0.35	–
Peak compressive strength ( $\sigma_{cp}$ , MPa)	20	400	–
Residual compressive strength ( $\sigma_{cr}$ , MPa)	3.5	–	–
Peak tensile strength ( $\sigma_{tp}$ , MPa)	3.1	500	–
Residual tensile strength ( $\sigma_{tr}$ , MPa)	0	–	–
Peak load (MN)	–	–	0.25
Residual load (MN)	–	–	0.025

**Table 8** The installed support units for the long-term stability

Support units	Portal slope	Cut slope
Shotcrete	Thickness: 15 cm	Thickness: 15 cm
Wire mesh	Type: Ø6.5 mm one layer	Type: Ø6.5 mm one layer
	Mesh spacing: 150 × 150 mm	Mesh spacing: 150 × 150 mm
Rock bolt	Type: Ø28 mm fully bonded	Type: Ø28 mm fully bonded
	Length: 6 m	Length: 6 m
	Spacing: 1.2 × 1.2 m	Spacing: 1.5 × 1.5 m

Finally, the finer zoning was applied to the analyzed models, and six-noded triangular finite elements were chosen in the mesh. Because the elastic-perfectly plastic (EPP) model best replicates the limit equilibrium analysis, the basaltic tuffs were considered to be EPP material. To understand the mechanism of the failure in the study area, the horizontal ground acceleration was not added into the analyses, when calculating the SRF values.

A SRF value of 1.50 was considered acceptable for the stability same as the limit equilibrium analysis. Based on the results of the numerical analyses, the SRF values of the portal and cut slopes were found to be 1.21 and 1.32, respectively (Fig. 8; Table 6). The results of the numerical stability analyses indicated that the mass movement on the portal slope was related to the composite failure starting with a circular surface and following a linear surface along the joint set J3 (Fig. 8a). However, the mass movement on the cut slope was connected with the circular failure (Fig. 8b). Even if any failure would not be expected to occur along the entire J3 surface based on the limit equilibrium analysis, the failure may occur because the rock mass has low strength parameters that comprise a circular surface where the mass leads to slide along the J3 according to the numerical analysis. Thus, some special measures were needed to prevent the effects of failures and to stabilize the area. The precautions to be taken are important for the safety and cost of the project. The support recommendations for the slopes are discussed in the later section.

### Reinforcement of the portal and cut slopes

Rock bolts, shotcrete, and wire mesh were selected as the reinforcement units for the slopes planned to be excavated. Their performance was also investigated by Phase<sup>2</sup> software using the SSR method. In addition, although there is not any seismic resource in and around the study area, the North Anatolian Fault zone crosses almost 200 km south of the area. For this reason, the minimum and possible horizontal ground acceleration was also considered, and it was taken to be 0.1 g for the long-term stability condition. After support installation, the SRF values increased from 1.21 to 1.63 for the portal slope (Fig. 9a), from 1.32 to 1.71 for the

cut slope (Fig. 9b), respectively. As a result, in case the proposed support units apply, the SRF values become higher than the acceptable SRF value of 1.50. The characteristics of the support units used in the numerical stability analyses are presented in Table 7 and installed support units for the long-term stability are given in the Table 8.

### Conclusions

In this study, an impending failure on nearby a residential area was investigated by kinematic, limit equilibrium, and numerical stability analyses. After the failure, a detailed field survey including drilling was performed, and the necessary data was obtained from the field and laboratory studies. The results obtained from these analyses can be summarized as follows:

- (a) The kinematic analyses results demonstrated that planar and wedge failures were possible on the portal slope, whereas no failure is expected on the cut slope. However, both planar and wedge failures were not expected to occur on the portal slope according to the limit equilibrium analysis, even for saturated conditions.
- (b) According to the findings of the numerical stability analyses based on the finite element method, composite and circular failures are possible on the portal and cut slopes, respectively.
- (c) All results showed that the landslide triggered by the excavations was not directly controlled by the joints. The circular failure on the cut slope might be related to the structure of dense fracture and low strength parameters of the rock mass, whereas for the portal slope, the failure mode is composite connected with both low strength parameters of rock mass and joints, the feasible measures were determined to make the region stable.
- (d) This study also shows that use of the different methods in studies where the stability of slopes are investigated, has a very important role in determination of occurrence mechanism of landslides, and realistic and reliable precautions.

**Acknowledgments** Authors would like to express their sincerest gratitude to the editor and reviewers for their excellent comments. Also thanks to MSc. Geology Engineer Aytuna Sayin from the Turkish General Directorate of Highways for the office work associated with this study.

## References

- Akgun A (2011) Assessment of possible damaged areas due to landslide-induced waves at a constructed reservoir using empirical approaches: Kurtun (North Turkey) dam reservoir area. *Nat Hazards Earth Syst Sci* 11(5):1341–1350
- Akgun A, Bulut F (2007) GIS-based landslide susceptibility for Arsin-Yomra (Trabzon, North Turkey) region. *Environ Geol* 51:1377–1387
- Akgun A, Dag S, Bulut F (2008) Landslide susceptibility mapping for a landslide-prone area (Fındıklı, NE of Turkey) by likelihood-frequency ratio and weighted linear combination models. *Environ Geol* 54:1127–1143
- Alemdag S, Kaya A, Karadag M, Gurocak Z, Bulut F (2013) Utilization of limit equilibrium method for the stability analysis of debris: an example of the Kalebasi District (Gumushane). *Cumhuriyet Earth Sci J* 30(2):49–62
- Alemdag S, Akgun A, Kaya A, Gokceoglu C (2014) A large and rapid planar failure: causes, mechanism and consequences (Mordut, Gumushane, Turkey). *Arab J Geosci* 7:1205–1221
- Alemdag S, Kaya A, Karadag M, Gurocak Z, Bulut F (2015) Utilization of the limit equilibrium and finite element methods for the stability analysis of the slope debris: an example of the Kalebasi district (NE Turkey). *J Afr Earth Sc.* doi:10.1016/j.jafrearsci.2015.03.010
- Barton N, Bandis SC (1990) Review of predictive capabilities of JRC-JCS model in engineering practice. *Proc Int Symp Rock Joints*, Loen 1990:603–610
- Bulut F, Boynukalin S, Tarhan F, Ataoglu E (2000) Reliability of landslide isopleth maps. *Bull Eng Geol Environ* 58:95–98
- CANMET (1977) Pit slope manual: supplement 5-1, plane shear analysis. Canada centre for mineral and energy technology report. 16–77
- Deere DU (1964) Technical description of rock cores for engineering purposed. *Rock Mech Rock Eng* 1:17–22
- Eberhardt ED (2003) Rock slope stability analysis—utilization of advanced numerical techniques. *Earth and Ocean sciences at UBC*
- Genc S (1993) Structural and geomorphological aspects of the Catak landslide, NE Turkey. *Q J Eng Geol Hydrogeol* 26(2):99–108
- Griffiths DV, Lane PA (1999) Slope stability analysis by finite elements. *Geotechnique* 49(3):387–403
- Gurocak Z, Alemdag S, Zaman M (2008) Rock slope stability and excavatability assessment of rocks at the Kapikaya dam site Eastern Turkey. *Eng Geol* 96(1–2):17–27
- Güven IH (1993) 1:250000-scaled geology and compilation of the Eastern Pontide. General directorate of mineral research and exploration (MTA) of Turkey, Ankara. (unpublished)
- Hammah RE, Yacoub TE, Curran JH (2006) Investigating the performance of the shear strength reduction (SSR) method on the analysis of reinforced slopes. In: *Proceedings of the 59th Canadian geotechnical conference*, Vancouver
- Hoek E, Bray JW (1981) *Rock slope engineering*. Institution of Mining and Metallurgy, London
- Hoek E, Diederichs MS (2006) Empirical estimation of rock mass modulus. *Int J Rock Mech Min Sci* 43:203–215
- Hoek E, Marinos P (2000) Predicting tunnel squeezing. *Tunnels and tunnelling international* 1-32(11):45–51, 2-32(12):34–36
- Hoek E, Carranza-Torres C, Corkum B (2002) Hoek-Brown failure criterion-2002 edition. In: *Proceedings of NARMS-TAC2002, mining innovation and technology*, Toronto, Canada, 267–273
- ISRM (2007) *The complete ISRM suggested methods for rock characterization, testing and monitoring: 1974–2006*. International Society of Rock Mechanics Turkish National Group, Ankara
- Karaman K (2013) Evaluation of rock slope stability by different methods (Unye, Ordu). *J Geol Eng* 37:27–47
- Karaman K, Ercikdi B, Kesimal A (2013) The assessment of slope stability and rock excavatability in a limestone quarry. *Earth Sci Res J* 17:169–181
- Karsli F, Atasoy M, Yalcin A, Reis S, Demir O, Gokceoglu C (2009) Effects of land-use changes on landslides in a landslide-prone area (Ardesen, Rize, NE Turkey). *Environ Monit Assess* 156:241–255
- Kaya A (2008) *The geotechnical investigation of the left tube's entrance portal of the Konakönü (Araklı-Trabzon) tunnel*. MSc Thesis, Karadeniz Technical University, Trabzon
- Kaya A, Bulut F, Alemdag S (2011a) Applicability of excavatability classification systems in underground excavations: a case study. *Sci Res Essays* 6(25):5331–5341
- Kaya A, Bulut F, Alemdag S, Sayin A (2011b) Analysis of support requirements for a tunnel portal in weak rock: a case study in Turkey. *Sci Res Essays* 6(31):6566–6583
- Kentli B, Topal T (2004) Assessment of rock slope stability for a segment of the Ankara-Pozanti motorway, Turkey. *Eng Geol* 74:73–90
- Kesimal A, Ercikdi B, Cihangir F (2008) Environmental impacts of blast-induced acceleration on slope instability at a limestone quarry. *Environ Geol* 54:381–389
- Kliche CA (1999) *Rock slope stability*. SME, Littleton
- Li X (2007) Finite element analysis of slope stability using a nonlinear failure criterion. *Comput Geotech* 34:127–136
- Mohr O (1900) Welche umstände bedingen die elastizitätsgrenze und den bruch eines materials? *Zeit des Ver Deut Ing* 44:1524–1530
- Nefeslioglu H, Gokceoglu C (2011) Probabilistic risk assessment in medium scale for rainfall-induced earthflows: Catakli catchment area (Cayeli, Rize, Turkey). *Math Probl Eng* 2011:1–21
- Nefeslioglu H, Gokceoglu C, Sonmez H, Gorum T (2011) Medium-scale hazard mapping for shallow landslide initiation: the Buyukkoy catchment area (Cayeli, Rize, Turkey). *Landslides* 8:459–483
- Osna T, Sezer AE, Akgun A (2014) GeoFIS: an integrated tool for the assessment of landslide susceptibility. *Comput Geosci* 66:20–30
- Reis S (2008) Analyzing land use/land cover changes using remote sensing and GIS in Rize, North-East Turkey. *Sensors* 8:6188–6202
- Reis S, Yalcin A, Atasoy M, Nisançi R, Bayrak T, Erduran M, Sancar C, Ekercin S (2012) Remote sensing and GIS-based landslide susceptibility mapping using frequency ratio and analytical hierarchy methods in Rize province (NE Turkey). *Environ Earth Sci* 66:2063–2073
- Rocscience (2004a) *Dips v5.0 graphical and statistical analysis of orientation data*. Rocscience Inc, Toronto
- Rocscience (2004b) *RocPlane v2.0 surface planar failure analysis*. Rocscience Inc, Toronto
- Rocscience (2004c) *Swedge v4.0 surface wedge analysis*. Rocscience Inc., Toronto
- Rocscience (2007) *Roclab v1.0 rock mass strength analysis using the generalized Hoek–Brown failure criterion*. Rocscience Inc, Toronto
- Rocscience (2008) *Phase<sup>2</sup> v7.0 finite element analysis for excavations and slopes*. Rocscience Inc, Toronto
- Shukra R, Baker R (2003) Mesh geometry effects on slope stability calculation by FLAC strength reduction method-linear and non-

- linear failure criteria. In: Brummer R et al (eds) Proceedings of the 3rd international FLAC symposium, Sudbury, Ontario, Canada, pp 109–116
- Topsakal E, Topal T (2015) Slope stability assessment of a re-activated landslide on the Artvin-Savsat junction of a provincial road in Meydancik. *Turk. Arab J Geosci* 8(3):1769–1786
- Turkish General Directorate of Highways (1997) List of specifications of the underground tunnel excavations with NATM practice (in Turkish). Turkish Ministry of Public Works, Ankara
- Turkish General Directorate of Highways (2006) Specification for highway works (in Turkish). Turkish Ministry of Public Works, Ankara
- Wyllie DC, Mah CW (2004) *Rock slope engineering*. Spon Press, NewYork
- Yalcin A (2008) GIS-based landslide susceptibility mapping using analytical hierarchy process and bivariate statistics in Ardesen (Turkey): comparisons of results and confirmations. *Catena* 72:1–12
- Yalcin A, Bulut F (2007) Landslide susceptibility mapping using GIS and digital photogrammetric techniques: a case study from Ardesen (NE-Turkey). *Nat Hazards* 41:201–226